

# Theoretical and Experimental Analysis of Electroporated Membrane Conductance in Cell Suspension

Daniela O. H. Suzuki, *Member IEEE*, Airton Ramos, Maria C. M. Ribeiro, Luisa H. Cazarolli, Fátima R. M. B. Silva, Laura D. Leite and Jefferson L. B. Marques, *Member IEEE*.

**Abstract**—An intense electric field can be applied to increase the conductivity of cell suspension and consequently, the membrane conductance ( $G_m$ ). This phenomenon is called *electroporation*. This mechanism is used in a wide range of medical applications, genetic engineering, and therapies. Conductivity measurements of cell suspensions were carried out during application of electric fields from 40 kV/m to 165 kV/m. Experimental results were analyzed with two electroporation models: the asymptotic electroporation model was used to estimate  $G_m$  at the beginning and at the end of electric field pulse, and the extended Kinoshita electroporation model to increase  $G_m$  linearly in time. The maximum  $G_m$  was  $1.7 \times 10^4$  S/m<sup>2</sup>, and the critical angle (when the  $G_m$  is insignificant) was 50 to 65 degrees. In addition, the sensitivity of electroporated membrane conductance to extracellular and cytoplasmic conductivity and cell radius has been studied. This study showed that external conductivity and cell radius are important parameters affecting the pore-opening phenomenon. However, if the cell radius is larger than 7  $\mu$ m in low conductivity medium, the cell dimensions are not so important.

**Index Terms**—Electroporation, membrane conductance, red blood cell, transmembrane potential, electric fields.

## I. INTRODUCTION

The cell membrane provides a selective barrier to the transport of ions and water-soluble molecules. When an

electric field is applied to a cell and the transmembrane voltage is increased to a critical value, there is structural conformation on the membrane and electropores appear [1]-[3]. This process is termed *electroporation*. The phenomenon permits the passage of ions, DNA, proteins, drugs, and impermeable substances into the cell [3]-[5].

The applied electric field produces accumulation of ions on the membrane faces and, as a consequence, a transmembrane voltage distribution ( $V_m$ ) is established. For a suspension of spherical cells of radius  $a$  and thickness  $h$  in a uniform electric field  $E$ ,  $V_m$  is given by:

$$V_m(t) = 1.5 g E a \cos \theta (1 - e^{-t/\tau}) \quad (1)$$

where  $\theta$  is the angle between the direction of the field and the position vector on the membrane (Fig. 1),  $g$  is a relative electric membrane permeability [6].

Kotnik *et al.* [6] presented the exact solution of Laplace's equation for a conducting spherical membrane in a uniform electric field. The authors derived the  $g$  value in the form:

$$g = \frac{\sigma_o [3ha^2\sigma_i + (3h^2a - h^3)(\sigma_m - \sigma_i)]}{a^3(\sigma_m + 2\sigma_o)(\sigma_m + 0.5\sigma_i) - (a-h)^3(\sigma_o - \sigma_m)(\sigma_i - \sigma_m)} \quad (2)$$

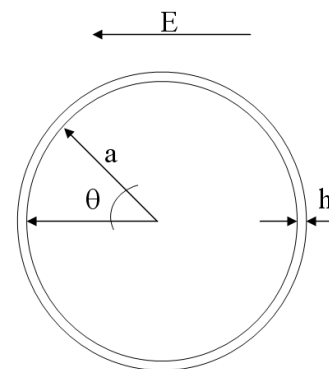


Fig. 1. Spherical cell with radius  $a$ , membrane thickness  $h$  in a uniform electric field  $E$ .  $\theta$  is the angle between the direction of the field and the position vector on the membrane.

Manuscript received March 30, 2010. This work was supported in part by the Conselho Brazilian Research Council (CNPq) under Grant 472484/2004-4.

D. O. H. Suzuki is with the Institute of Biomedical Engineering, Department of Electrical Engineering, CTC, UFSC, CEP 88040-900, Florianópolis-SC, Brazil (e-mail: [suzuki@ieb.ufsc.br](mailto:suzuki@ieb.ufsc.br)).

A. Ramos is with Biomedical Engineering Group, Department of Electrical Engineering, CCT, UDESC, 88223-100, Joinville-SC, Brazil (e-mail: [dee2ar@joinville.udesc.br](mailto:dee2ar@joinville.udesc.br)).

M.C.M. Ribeiro is with Department of Molecular Biology, Embryology and Genetics, CCB, UFSC, 88040-900, Florianópolis-SC, Brazil (e-mail: [menks@ccb.ufsc.br](mailto:menks@ccb.ufsc.br)).

L. H. Cazarolli is with Department of Biochemistry, CCB, UFSC, 88040-900, Florianópolis-SC, Brazil (e-mail: [luisacazarolli@gmail.com](mailto:luisacazarolli@gmail.com)).

L. D. Leite is with Department of Physiology, CCB, UFSC, 88040-900, Florianópolis-SC, Brazil (e-mail: [laura@ccb.ufsc.br](mailto:laura@ccb.ufsc.br)).

F. R. M. B. Silva is with Department of Biochemistry, CCB, UFSC, 88040-900, Florianópolis-SC, Brazil (e-mail: [mena@mbox1.ufsc.br](mailto:mena@mbox1.ufsc.br)).

J. L. B. Marques is with the Institute of Biomedical Engineering, Department of Electrical Engineering, CTC, UFSC, 88040-900, Florianópolis-SC, Brazil (e-mail: [jmarques@ieb.ufsc.br](mailto:jmarques@ieb.ufsc.br)).

and the time constant  $\tau$ :

$$\tau = \frac{aC_m}{\frac{2\sigma_o\sigma_i}{2\sigma_o + \sigma_i} + \frac{a}{h}\sigma_m} \quad (3)$$

$\sigma_m$ ,  $\sigma_i$ , and  $\sigma_o$  are the conductivity of the membrane, cytoplasm, and outer media, respectively;  $C_m$  is the membrane capacitance (per unit area). For  $\sigma_m=0$  (intact membrane),  $g=1$ .

When the induced transmembrane potential exceeds 200 mV to 1 V [3]-[5], pores are formed. The electroporation introduces  $\sigma_m \neq 0$ . Some experimental and theoretical work estimated the electroporated membrane conductance ( $G_m = \sigma_m/h$  [7]) at about  $10^4$  S/m<sup>2</sup> [6], [8]. However, Hibino *et al.* [9] presented estimated values in the range from  $2 \times 10^4$  S/m<sup>2</sup> to  $10^5$  S/m<sup>2</sup>. Pavlin *et al.* [10], [11] showed theoretical studies of effective conductivity of a suspension of cells, using  $G_m = 8 \times 10^4$  S/m<sup>2</sup>.

The electroporation phenomenon is not yet completely understood or explained. Therefore, to bridge this gap, several authors have been developing theoretical electroporation models to study the cell membrane conductance. The models of pore energy [12] were used with Smoluchowsky equation to provide pore distribution [13]-[15]. Glaser *et al.* [16] presented an electroporation model as a function of time, with a rate of change in  $G_m$  depending on the applied voltage. This work presented good agreement with the planar membrane experiments. Later work by Ramos *et al.* [17], [18] extended the Glaser electroporation model [16] in the study of spherical cells and tissue. Kinoshita *et al.* [19] described a membrane conductance model based on voltage-sensitive fluorescence experiments. Neu *et al.* [15] and De Bruin *et al.* [20] proposed an asymptotical model to describe the pore opening and resealing dynamics.

This work measures the electric conductivity of a cell suspension under applied electric fields of 40 to 165 kV/m, with volumetric fraction of  $p=0.07$ . The modification of cell suspension conductivity was made to compare the asymptotic and Kinoshita's model with experimental data. The original asymptotic model [15], [20] was used to study at the beginning and at the end of electroporated membrane conductance during the pulse [21]. Kinoshita's electroporation model was used to analyze the linear increase of membrane conductance ([1], [14], [23]) from 100  $\mu$ s to 400  $\mu$ s during a 500  $\mu$ s electroporation pulse. The Krassowska *et al.* model [22] was used to compare with experimental data at 100  $\mu$ s. Kinoshita's model was improved by introducing a new equation to provide continuous time analysis. Not only was the behavior of the cell membrane conductance verified numerically during electroporation pulses, but also the effect of the electrolyte, cytoplasm conductivity, and cell dimensions

on the electroporated membrane conductance in cell

TABLE I  
GEOMETRIC AND ELECTRICAL PARAMETERS APPLIED TO  
NUMERICAL RESULTS USING KINOSHITA'S ELECTROPORATION  
MODEL

Symbol	Description	Value
$\sigma_o$	external conductivity	0.23 S/m
$\sigma_i$	internal conductivity	0.62 S/m [24]
$p$	volumetric fraction	0.07
$h$	membrane thickness	$7 \times 10^{-9}$ m

suspension.

## II. MATERIAL AND METHODS

### A. Cell Preparation

Erythrocytes were obtained from male albino wistar rats blood (160–190 g) after centrifugation by removing the buffy coat. The conductivity of cell suspensions was measured on the same day of blood collection after washing two times with isotonic low ionic strength solution (ILISS), composed of 13 mM NaCl, 150 mM sucrose, 14 mM NaOH, pH 7.4 [2]. Spherical erythrocytes (spherocytes) were prepared in 67% of ILISS,  $\sigma_o=0.23$  S/m at 23°C (conductometer Metrohm mod. 712, Herisau, Switzerland). The spherocytes can eliminate morphological complication in theoretical analysis [24]. The mean spherocyte diameter was  $3.2 \pm 0.6$   $\mu$ m. Cell diameters were measured with an Olympus BX41 microscope equipped with an Olympus Qcolor 3 digital camera (Olympus America, Inc., Melville, NY) and using a QCapture Pro (Media Cybernetics, Inc., Surrey, BC, Canada); no change in cell size was observed after 10 minutes. Erythrocyte suspensions with cell volume fractions  $p=0.07$  ( $0.51 \times 10^6$  cells/ml) were used in the experiments. Conductivity measurements were carried out on three experiments on two different days. All the animals were carefully monitored and maintained in accordance with ethical recommendations of the Brazilian Veterinary-Medicine Council and the Brazilian College of Animal Experimentation.

### B. Conductivity Measurements

A computer program and an electroporator to supply high-voltage square pulses were developed. The suspended red cells were sandwiched between stainless steel plates of 5 mm $\times$ 5 mm $\times$ 2 mm dimension. Electric fields of 40 kV/m to 165 kV/m were used for duration of 500  $\mu$ s. The measurements of the electric current and the potential during the pulse were obtained using a current probe (Tektronix A622, Beaverton, Oregon, USA), high-voltage probe (Tektronix P5102, Beaverton, Oregon, USA), and digital oscilloscope (Tektronix THS720A, Beaverton, Oregon, USA). These results were recorded, transmitted to a computer, and low-pass filtered (digital, zero phase, 4th order Butterworth) at 100 kHz. The experiments were performed at 23°C. The

conductivity measurement of the medium with no cells (ILISS) was obtained before each experiment. In independent experiments, fluorescent dyes (FITC-dextran 250S, Sigma Chemical Co., St. Louis, MO) were introduced and the suspension conductivity was measured. At this volumetric fraction of cells ( $p=0.07$ ), electroporation produces measurable suspension conductivity changes; this was confirmed by the appearance of a fluorescent dye in the cells (data not shown). Cell viability was assessed after the electroporation pulse and it showed around 70% survival rate for electric field strongest than 100kV/m.

### C. Theoretical Analysis of Membrane Conductance: Kinoshita's Electroporation Model

The membrane conductance ( $G_m$ ) increases when the transmembrane potential is stronger than a critical value. The ionic transport through the membrane was suggested by Kinoshita *et al.* [19]. The authors analyzed the cell images using a fluorescent dye. The equation (4) considers the symmetry for  $G_m$  on the cell. The electroporated membrane conductance, for  $0 \leq \theta \leq \theta_c$  and  $(180^\circ - \theta_c) \leq \theta \leq 180^\circ$ , is:

$$G_m(\theta) = G_{mo} \frac{(\cos \theta - \cos \theta_c)}{(1 - \cos \theta_c)} \quad (4)$$

$\theta_c$  is the critical angle at which the transmembrane potential, in the absence of pores, is equal to the critical value. When  $0 \leq \theta \leq (180^\circ - \theta_c)$ ,  $G_m(\theta) = 0$ .  $G_{mo}$  is the maximum conductance of the electroporated membrane ( $\theta = 0$  and  $180^\circ$ ).

Kinoshita's model presents analysis at a discrete point in time; it does not consider the evolution of pores and transmembrane potential. Equation (5) was proposed to introduce the dynamic electroporation on equation (4):

$$G_m = A(t) \cdot V_{mo}^2 + B(t) \quad (5)$$

where  $V_{mo}$  is the transmembrane potential to intact membrane at the cell pole, equation (1) ( $g=1$ ,  $\theta=0^\circ$ ). Glaser *et al.* [16] verified that planar lipidic membranes excited by electric field pulses increase their conductance with time, having a rate depending on the applied voltage. This dependence was observed to follow a well-defined rule,  $\ln(\Delta I_m / \Delta t) = A V_m^2 + B$ , where  $V_m$  and  $I_m$  are the transmembrane voltage and current, respectively, and  $\Delta t$  is the time length of the pulse. The constants  $A$  and  $B$  were determined for membranes of asolectin [16]. The equation (5) suggests that the ionic mobility in an electroporated membrane increases on a rate depending on the transmembrane voltage. Glaser *et al.* [16] use simplified descriptions of the electroporation process to interpret the collected data. This model proposes a variation of  $A(t)$  and  $B(t)$  to introduce the increase of membrane conductance during the electroporation.

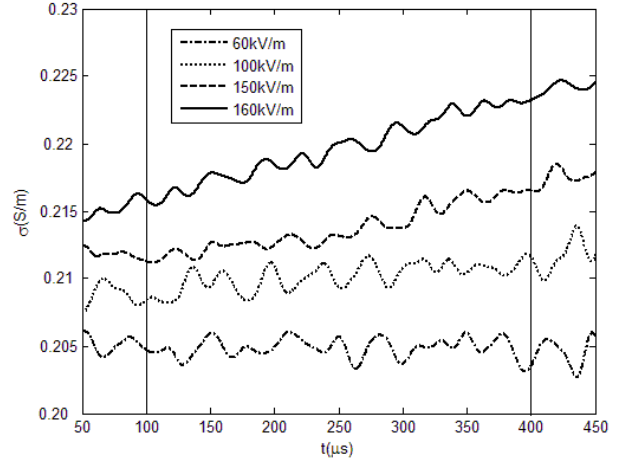


Fig. 2. Conductivity of cell suspension ( $p=0.07$ ) during pulses of 500  $\mu$ s. The conductivity change with pulses of 100 kV/m and over. Vertical lines show the limit of satisfactory curves between 100 and 400  $\mu$ s.

The cell suspension conductivity, for diluted solutions, using the Maxwell model [10] is:

$$\frac{\sigma_o - \sigma}{2\sigma_o + \sigma} = p \cdot \frac{\sigma_o - \sigma_p}{2\sigma_o + \sigma_p} \quad (6)$$

where  $\sigma$  and  $\sigma_o$  are the cell suspension and the external conductivity.  $\sigma_p$  is the cell conductivity:

$$\sigma_p = \sigma_m \frac{2(1-\xi)\sigma_m + (1+2\xi)\sigma_i}{(2+\xi)\sigma_m + (1-\xi)\sigma_i}, \quad (7)$$

$$\xi = \left(\frac{1-h}{a}\right)^3$$

$\sigma_m$  is the membrane conductivity ( $G_m = \sigma_m / h$  [7]). The parameters used in this model are presented in Table I.

### D. Theoretical Analysis of Membrane Conductance: Asymptotic Electroporation Model

For an isolated spherical cell under a uniform electric field  $E$ ,  $t=0$  was applied. The Laplace equation was solved with azimuthal symmetry,  $a \gg h$ . The following boundary conditions were considered:

$$\begin{aligned} \sigma_o \cdot \frac{\partial \varphi_o}{\partial r}(a) + \epsilon_w \cdot \frac{\partial}{\partial t} \frac{\partial \varphi_o}{\partial r}(a) &= \\ \sigma_i \cdot \frac{\partial \varphi_i}{\partial r}(a) + \epsilon_w \cdot \frac{\partial}{\partial t} \frac{\partial \varphi_i}{\partial r}(a) &= G_m \cdot V_m + C_m \cdot \frac{\partial V_m}{\partial t} \\ \varphi_i(r=0) &\rightarrow \text{finite} \\ \varphi_o(r \rightarrow \infty) &= -r \cdot E \cos \theta \end{aligned} \quad (8)$$

TABLE II  
GEOMETRICAL CHARACTERISTICS, ELECTRICAL PROPERTIES, AND  
PARAMETERS OF THE ASYMPTOTIC MODEL

Symbol	Description	Value
$r_p$	pore radius	$0.75 \times 10^{-9}$ m [20]
$V_p$	electroporation threshold voltage	$200.10^{-3}$ V [33]
$V_i$	at $T=300$ K	$26.10^{-3}$ V
$w_o$	Energy barrier within pore	$70.10^{-3}$ V [20]
$p_r$	Relative entrance length of pore	0.15 [20]
$\alpha$	electroporation parameter	$4.10^{19}$ m <sup>2</sup> .s <sup>-1</sup>
$q$	electroporation parameter	3.48
$N_o$	pore number per unit area when $V_m=0$	$10^9$ m <sup>-2</sup> [20]
$C_m$	membrane capacitance	$8 \times 10^{-3}$ F.m <sup>-2</sup> [27]

where  $\epsilon_w$  is the water permittivity,  $\phi_o$  and  $\phi_i$  are the cell's internal and external electric potentials, respectively. The transmembrane potential ( $V_m = \phi_o(a) - \phi_i(a)$ ) in time domain can be solved with the solution of equation (9) :

$$\frac{dV_m}{dt} + \alpha V_m = -kE \quad (9)$$

where

$$\alpha = \frac{G_m + \frac{C_m}{\tau_o}}{C_m + C_w}$$

$$k = \frac{1.5a \cos \theta}{\left( \tau_o + \frac{\epsilon_w}{\sigma_i} \right)}$$

$$C_w = \frac{\epsilon_w}{a \left( 1 + \frac{\sigma_i}{2\sigma_o} \right)}$$

The time constant is:

$$\tau_o = a C_m \left( \frac{1}{\sigma_i} + \frac{1}{2\sigma_o} \right) \quad (10)$$

The asymptotic electroporation model in [15], [20] was used for studying the electroporated membrane conductance:

$$G_m = N_p G_p \quad (11)$$

$G_p$  is conductance in a single pore.  $N_p$  is the pore number per unit area:

$$\frac{\partial N_p}{\partial t} = \alpha e^{(V_m/V_p)^2} \left[ 1 - \frac{N_p}{N_o} e^{-q(V_m/V_p)^2} \right] \quad (12)$$

where  $N_o$  is the pore density when  $V_m=0$ .  $V_p$  sets the critical transmembrane potential at which the membrane breakdowns.  $\alpha$  and  $q$  are electroporation constants. These two parameters were optimized for the best fit experimental values (Table II).

The pore conductance  $G_p$  is a function of transmembrane potential:

$$G_p = \left( \frac{\pi r_p^2 (\sigma_i + \sigma_o)}{h} \right) e^{V_m/V_i} - 1 \quad (13)$$

$$\left[ \frac{w_o e^{-\frac{w_o - p_r V_m}{V_i}} - p_r V_m}{w_o - p_r V_m} \right] e^{V_m/V_i} - \left[ \frac{w_o e^{-\frac{w_o + p_r V_m}{V_i}} + p_r V_m}{w_o + p_r V_m} \right]$$

$p_r$  is a relative pore length,  $V_i = kT/e$ , where  $k$  is Boltzmann's constant,  $T=300$ K, and  $e$  is the elementary charge. The pore radius  $r_p=0.75$  nm agrees with the minimum pore established by molecular dynamics (0.7 nm) [26]. The geometrical and the electrical parameters used in asymptotic model are presented in Tables I and II.

The proximity of the cells produces a reduction of transmembrane potential and suspension conductivity [8], [28]-[30]. The influence of neighboring cells was considered negligible. The decrease of the induced transmembrane potential was calculated to be about 3% for  $p=0.07$  [28].

### E. Numerical Implementation

A program has been developed in C++ language for a PC-compatible platform running the Windows XP operational system.. Simulations were carried out to obtain the numerical solutions for the equations.

The conductivity of suspensions,  $\sigma$ , has been calculation using the equations (5) and (6). The theoretical models results were fitted to experimental suspension conductivity. The electroporation models depend on transmembrane potential.  $V_m$  has to be calculated according to equation (9) and (10). When  $V_m > 200$  mV [3, 4], the  $G_m$  increase and creates pathways across the cell membrane. This ionic diffusion through the membrane decreases  $V_m$  and consequently  $G_m$ .

The equation (4) has been used to implement the Kinosita's model. The parameters of the model are in Table I. The alteration of the membrane conductance by asymptotic model has been implemented using the equation (11), (12) and (13). The differential equations are solved by finite differential method. The time step used was specified as 65ps. The cell is divided into segments of  $\Delta\theta=0.032$  rad. The applied electric field was a pulse of 40 to 165 kV/m. It has also been assumed that at time  $t = 0$ , assume  $G_m = 10$  S/m<sup>2</sup> [6]  $V_m = 0$ ,  $N_p = N_o$ .  $N_o$  is the equilibrium pore density at  $V_m = 0$  and depends on the rate of thermal fluctuations of lipid

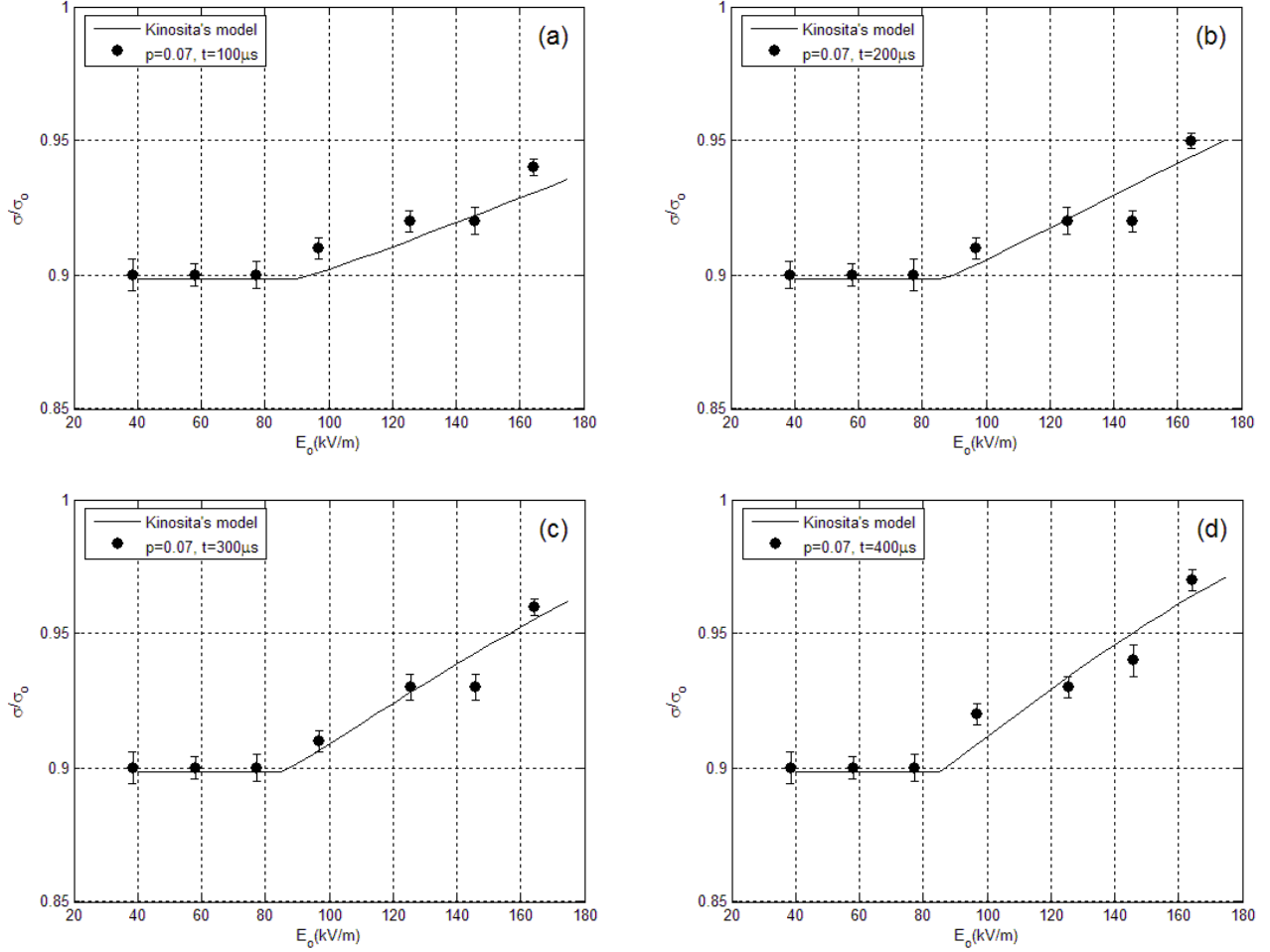


Fig. 3. Normalized conductivity suspension as a function of the different electric fields at (a) 100  $\mu\text{s}$ , (b) 200  $\mu\text{s}$ , (c) 300  $\mu\text{s}$ , and (d) 400  $\mu\text{s}$ . The points are the experimental data. The solid line is the numeric simulation of single spherical cell with Kinosita's electroporation model, equation (5),  $A(t)=3.4t+33\times 10^{-4} \text{ A}\cdot\text{V}^{-3}\cdot\text{m}^{-2}$  and  $B(t)=-4.9\times 10^7 t-33\times 10^4 \text{ S/m}^2$  and  $\theta_c=50^\circ$ . The maximum error between experimental and theoretical is 3%. Mean and standard deviation values of three experiments.

molecules in the membrane. The parameters of the asymptotic model are in Table II.

### III. RESULTS

Fig. 2 presents the measured results of cell suspension conductivity,  $\sigma(t)=I(t)/U(t)\cdot d/S$ , where  $d$  is the distance between plates and  $S$  the surface of the sample volume at the plates. The digital filter introduced overshoots at the beginning and the end of the pulse. Then, satisfactory results between 100 to 400  $\mu\text{s}$  were considered. Fig. 2 shows the cell suspension conductivity depends on the electric field intensity.

Comparing the experimental and the theoretical results of cell suspension conductivity, the following is obtained:  $A(t)=3.4t+33\times 10^{-4} \text{ A}\cdot\text{V}^{-3}\cdot\text{m}^{-2}$  and  $B(t)=-4.9\times 10^7 t+33\times 10^4 \text{ S/m}^2$  (Fig. 3). The  $\theta_c$  variation from  $45^\circ$  to  $70^\circ$  [9] produces a maximum error of 3%.

Kinosita's electroporation model was used to verify the conductivity dependence on critical angle and maximum conductance,  $E_o=160 \text{ kV/m}$  (Fig. 4). The distribution spatial

possibilities of  $G_m$  on cellular membrane were analyzed with this graphic. This result towards understanding the mechanism of electroporation.

Fig. 5 shows the comparison of cell suspension conductivity between theoretical ( $\blacksquare$ ) and experimental ( $\bullet$ ) data. The experimental points were obtained at 100  $\mu\text{s}$ . These results were of cell suspensions with  $p=0.07$ ,  $\sigma_o=0.23 \text{ S/m}$ ,  $\sigma_i=0.62 \text{ S/m}$  [24], and  $a=3.2 \mu\text{m}$ . The errors between the theoretical and the experimental curves account for less than 1%. The parameters  $\alpha$  and  $q$  used are  $4\cdot 10^{19} \text{ m}^{-2}\cdot\text{s}^{-1}$  and 3.48, respectively.

The transmembrane potential increase according the equation (1), when  $V_m$  exceeds a critical value ( $V_c$ ), there are the creation of pores and  $G_m$  increases. The asymptotic model describes the behavior of pore creation and destruction [15], [20]. The spatial and time dynamics of membrane conductance when the electric field was applied and then turned off are shown in Figs. 6 and 7. The maximum values of  $G_m$  were near the pole. When the electric field was turned off,  $G_m$  decreases very fast.

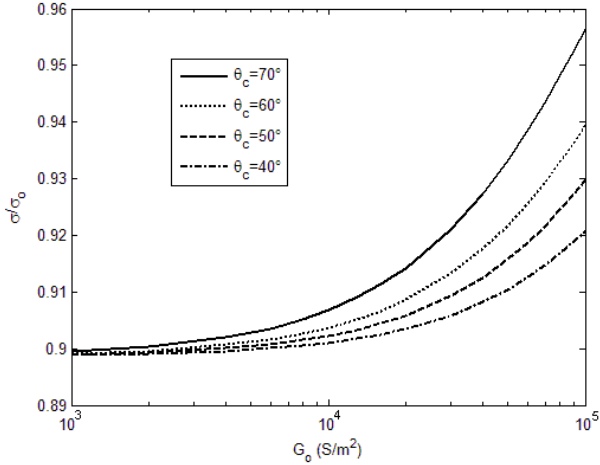


Fig. 4. Dependence of the normalized conductivity to the electroporated membrane conductance on the pole. The variation of the  $\theta_c$  from  $40^\circ$  to  $70^\circ$  using Kinosita's electroporation model was observed.

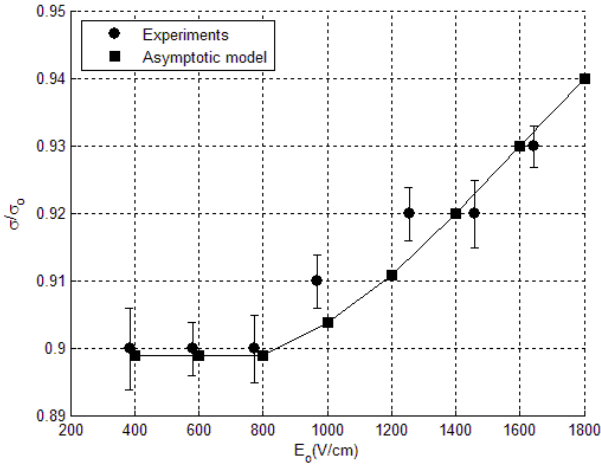


Fig. 5. Normalized cell suspension conductivity for different electric fields. The dots are the experimental results (at  $100\mu\text{s}$ ). The squares represent the numerical result of a single spherical cell with asymptotic electroporation model. The solid line is the trend of the simulation results. The numerical model parameters are  $p=0.07$ ,  $\sigma_o=0.23\text{ S/m}$ ,  $\sigma_e=0.62\text{ S/m}$  [24], and  $a=3.2\mu\text{m}$ . Mean and standard deviation values of three experiments.

The influence of variations of external and internal conductivity and cell radius, within the range of physiological values, presented significant alterations in electroporated membrane conductance (Figs. 8, 9, and 10). The results presented are important for the design and understand of electrical protocols for cell electroporation.

#### IV. DISCUSSION AND CONCLUSIONS

The conductivity of the suspension is reduced by proximity of the cells. The measured suspension conductivity for 40 to 80 kV/m shows a reduction of 10% of medium without cells (Fig. 2, 3, and 5). This value is consistent with the Maxwell model, theoretical [29], and experimental reports [8], [11].

The morphological alteration of erythrocytes to spherical form produce lateral membrane tension. This effect decreases

the critical transmembrane potential ( $V_c$ ) to trigger membrane electroporation [31]. Barrau *et al.* [31] demonstrated that a 100 mV reduction on critical transmembrane potential is

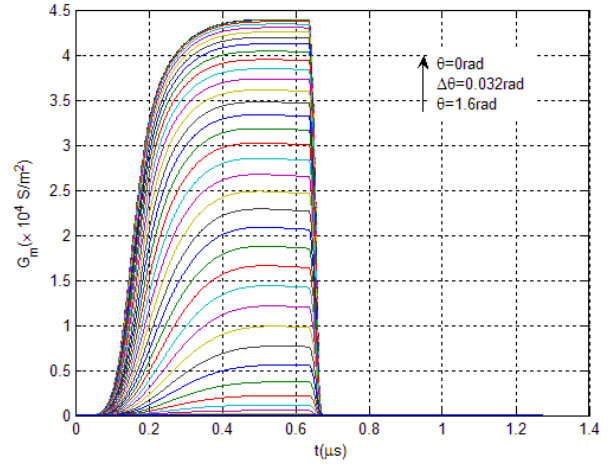


Fig. 6. Dynamic membrane conductance using asymptotic electroporation model in time for  $0 \leq \theta \leq 1.6\text{ rad}$ ,  $\Delta\theta=0.032\text{ rad}$ . At  $t=0$ ,  $E=130\text{ kV/m}$  is applied. After  $0.65\mu\text{s}$ , the electric field is turned off.

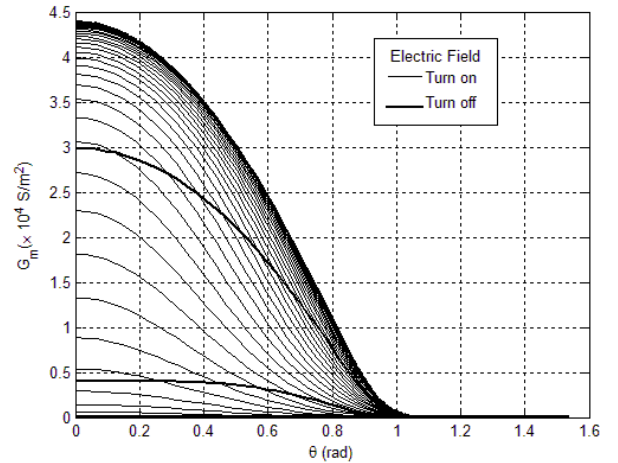


Fig. 7. Angular distribution of electroporated membrane conductance during on (thin line) and off (bold line) intervals.  $\Delta t=1.3\text{ ns}$ ,  $E=130\text{ kV/m}$ , asymptotic electroporation model.

associated with osmotic pressure decrease of 43%. An imprecision of 50 mV on critical transmembrane potential was considered, corresponding to the 33% reduction in osmotic pressure of the external medium. There was an increase in suspension conductivity during application of electric fields above 100 kV/m. Using the equation (1) we obtained  $V_c=460\text{ mV}$ . Similar results were obtained by Pavlin *et al.* [10], where the volumetric fraction was  $p=0.30$ . These increases on the conductivity above threshold electric field agree with other groups [5], [32], [33]. The measured suspension conductivity presented an insignificant alteration considering the minimum threshold of critical transmembrane potential of 200 mV [34].

Good agreement is obtained between experimental and

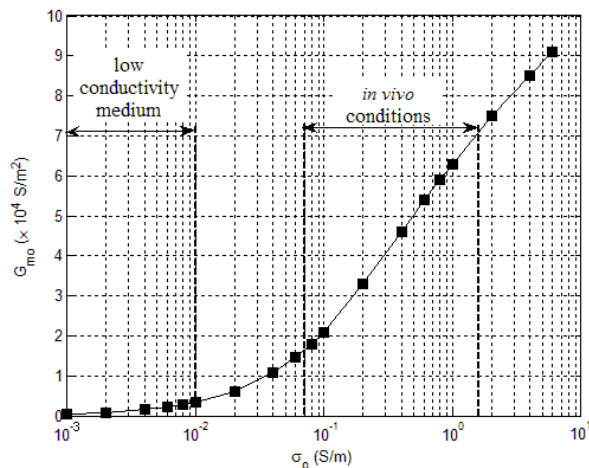


Fig. 8. Effect of external conductivity on maximum conductance of electroporated membrane at steady state ( $G_{mo}$ ). The numerical results were simulated with asymptotic model,  $E=120$  kV/m,  $\sigma_i=0.62$  S/m and  $a=3.2$   $\mu\text{m}$ .

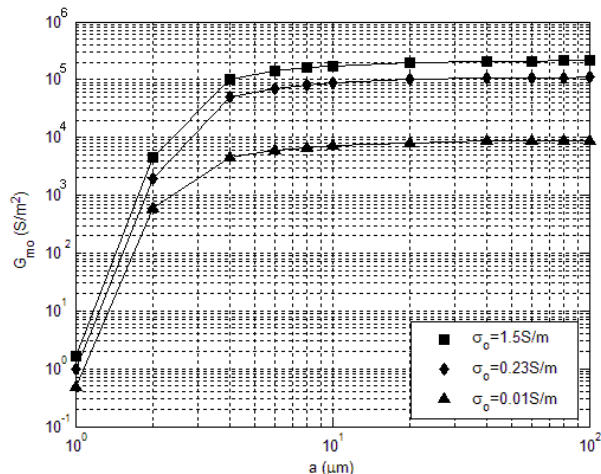


Fig. 10. Influence of cell dimension on the maximum conductance of electroporated membrane at steady state.  $E=120$  kV/m,  $\sigma_i=0.62$  S/m, asymptotic electroporation model.

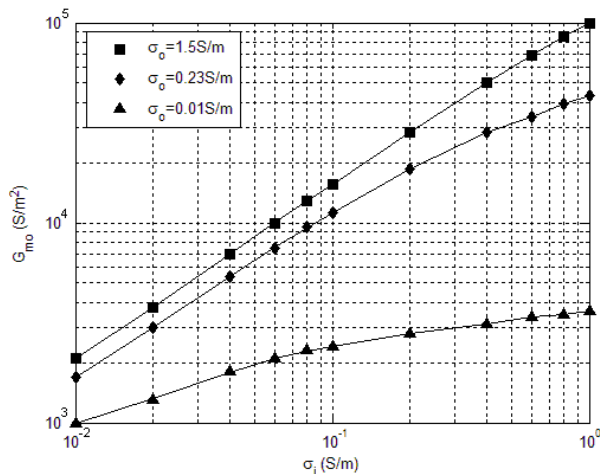


Fig. 9. Dependence of the maximum conductance of electroporated membrane at steady state to the internal conductivity.  $E=120$  kV/m,  $a=3.2$   $\mu\text{m}$ , asymptotic electroporation model.

theoretical results for Kinosita's model (Fig. 3) and asymptotic model (Fig. 4), errors being less than 3% and 1%, respectively. The electroporated membrane conductance for both models is similar to the results obtained by other authors [8], [9], [15], [35], [36]. The angular variation of asymptotic model (from  $51^\circ$  to  $63^\circ$ , Fig. 7) agrees with the experimental data using fluorescent microscopy [9].

For values of  $\theta_c \leq 40^\circ$ , the increase in electroporated membrane conductance is lowest (Fig. 4). Also,  $G_{mo}$  must be higher than the values reported in the literature ( $10^4$ - $10^5$  S/m<sup>2</sup> [8], [15], [35], [36]) to provide  $\sigma/\sigma_o \geq 0.92$  obtained experimentally. However, in the experiments, at 400  $\mu\text{s}$  (Fig. 2)  $\sigma/\sigma_o \geq 0.95$  was observed. Then, the electroporation pores might cover a membrane area more than 33% ( $\theta_c \geq 40^\circ$ ). Analysis of Fig. 3 suggests that rat erythrocytes, exposed to applied electric fields above 150kV/m, produced intense

alteration of membrane conductance at cell pole, and a significant membrane area was affected. With  $G_{mo}=10^5$  S/m<sup>2</sup> and  $\theta_c=70^\circ$ , the theoretical model values were compatible with the experimental results of Fig. 3(d).

Different electroporation parameters  $\alpha$  and  $q$  were found for the asymptotic model from DeBruin *et al.* [20] and Stewart *et al.* [37], Table II. Another parameter altered from the original asymptotic model was the electroporation threshold voltage ( $V_p$ ). Teissié *et al.* [33] performed experiments with different cells and proposed 200 mV for the critical transmembrane potential. The different asymptotic model parameters as compared to the DeBruin *et al.* [20] (experimental results from artificial bilayers [16]), Stewart *et al.* [37] studies (space-clamp and voltage-clamp) and this work (suspensions conductivity) may be caused by indirect techniques of electroporation effects. Quantitative variations of parameters could be caused by indirect measure of electroporation phenomena. Though the equations of asymptotic model remain the same for these works.

Stewart *et al.* [37] increased the pore radius (from 0.75 nm to 20 nm) to fit the mathematical model and the experiments with muscle cell. The pore conductance on asymptotic model was obtained from experimental studies. This model considers the Born energy to be a (trapezoidal) barrier to ion passage through the pore [16], [20]. When the pores are larger than 5 nm, this barrier is insignificant. So, the pore conductance is represented by two resistances connected in series [1], [22]. The original asymptotic model was not useful with large pores.

The experimental findings (Fig. 2) and equation (5) of this study are consistent with Wilhelm *et al.* [38] and Kroeger *et al.* [39] indicating that membrane conductance increases linearly with time. This suggests that transmembrane potential is an overcritical value; this is the "expansion step" described by Teissié *et al.* [3] based on experimental

observations suggesting five electroporation stages: Induction, the electric field induces transmembrane potential increase until the critical potential (about 200 mV [34]); Membrane rupture produces structural rearrangement from hydrophobic to hydrophilic pores [1]; Expansion, pore evolution; Stabilization, the transmembrane potential is subcritical and there is no increase in pore numbers and size; Resealing, resealing of pores; and Memory, the membrane property modifications remain on for long time (hours).

Based on electroporation theory [1]-[4] and Figs. 2, 3, 6, and 8, electroporation membrane conductance dynamic may be divided into two phases: PORE OPENING, including (1) membrane conductance increase, mainly at cell pole with rapid scattering of pores in the membrane; (2) membrane conductance grows linearly; (3)  $G_m$  becomes constant, number and distribution of pores are invariable. PORE RESEALING: (4)  $G_m$  decreases quickly.

Step (1) presents difficult experimental confirmation, because it happens in less than 1  $\mu$ s [1], [3], [9]. Step (2) was verified through a linear increase of membrane conductance in time based on experimental results (from 100  $\mu$ s to 400  $\mu$ s) and Kinoshita's model (Fig. 3 and equation (5)). The equation indicates the relation between the membrane conductance and the quadratic-induced transmembrane potential. It is consistent with the other electroporation models [16], [20]. Step (3) presents the limitation of the asymptotic model. Some authors [1], [2] describe step (3) like the stabilization of pores. The experiments of this work did not show this effect.

The resealing of pores (step 4) presents the rapid relaxation of conductivity experimentally [11] and with the asymptotic model (Fig. 6). However, it disagrees with the hypothesis that long-lived pores increase the membrane permeability for ions and molecules, minutes after the electric pulse is turned off [39]. One possible explanation for this is that long-lived pores (40 ms after the electric pulse turn-off [39]) formed due to the intense electric field (400 kV/m - 500 kV/m) applied. These values are stronger than electric field used in this work. The issues discussed provide evidence that very strong electric field overcomes an energy barrier allowing the creation of long-lived pores, although this energy stage is not described by current models [1], [12]. The molecular alteration caused in membrane structure will persist for a long time [1], [3], [4].

Fig. 8 shows the increase in membrane conductance, mainly *in vivo* conditions. However, the variation of electroporated cell membrane conductance ( $G_{mo}$ ), in low conductivity medium, is much smaller than *in vivo* conditions. This effect is stronger with larger cells because the transmembrane potential is proportional to cell radius, equation (1).

The internal cell characteristics, *e.g.*, organelles, produce different internal conductivity. The increase of membrane conductance in a low internal conductivity medium is insignificant (Fig. 9), although the influence of

internal conductivity on  $G_{mo}$  is noted in high external conductivity medium.

The numerical analysis using spherical cells, Fig. 10, shows the dependence of  $G_{mo}$  with cell dimensions. For small cells ( $a < 4 \mu$ m; *e.g.*, bacteria), size variations less than 1  $\mu$ m produce differences in membrane conductance of 10 times. The  $G_{mo}$  variation is smaller for large cells (*e.g.*, sea urchin eggs [19]).

In the same cell suspension, the electric fields did not produce the same effect in all cells. It may be caused by different cell sizes in the same sample. In the experiments performed in this review, variations of cell diameter from 2.6  $\mu$ m to 3.8  $\mu$ m were observed and produced  $G_m$  from  $0.5 \times 10^4$  S/m<sup>2</sup> to  $4 \times 10^4$  S/m<sup>2</sup>, respectively (Fig. 10). This observation suggests that in the same cell suspension cells with large pores, low membrane permeability, and irreversible electroporation (cell death) can be observed.

Unfortunately, the methodology developed does not provide information on size and number of pores. Another problem is that dense cell suspension and intense electric fields ( $p > 0.20$  and  $V_m > 300$  mV) produce an increase in cell suspension conductivity [41], [42]. In addition, suspension conductivity may be influenced with long pulses causing cell electrophoresis [43]. In the experiments carried out in this study, this effect was reduced by diluting the cell suspension ( $p = 0.07$ ) [41], [44].

This work carried out experiments to obtain the alteration of conductivity in a dilute cell suspension during electroporation pulses. Two electroporation models were used to analyze these experimental results. A linear equation (equation (5)) for membrane conductance at the "expansion step" on Kinoshita's model was included. The electroporated membrane conductance of this numerical analysis is similar to previous results [8], [15], [34], [35]. With the parameters from the experiments, the asymptotic model shows that cell dimension, and external and internal conductivity are important parameters to consider, as well as the intensity and the duration of electroporation pulses. However, cells with diameters greater than 7  $\mu$ m in low conductivity medium show no increase in electroporated membrane conductance. The numerical results of electroporation dynamics demonstrate that at the beginning the pores are concentrated on cell pole; later on pores cover over 30% of the total membrane area.

#### ACKNOWLEDGMENTS

The Brazilian research council (CNPq) is acknowledged for the project research grant and D.O.H.S. scholarship. The authors wish to express their appreciation to Dr. Haidi Fiedler and Dr. Faruk Nome for their experimental support.

#### REFERENCES

- [1] J. C. Weaver, and Y. A. Chizmadzhev, "Theory of electroporation: A review," *Bioelectrochemistry*, vol. 41, pp.135-160, Dec. 1996.

- [2] D. C. Chang, "Structure and dynamics of electric field induced membrane pores as revealed by rapid-freezing electron microscopy," in *Guide to Electroporation and Electrofusion*, D. C. Chang, B. M. Chassy, J. A. Saunders, and A. E. Sowers, San Diego, CA: Academic Press, 1991, pp. 9-27.
- [3] J. Teissié, M. Golzio, and M. P. Rols, "Mechanisms of cell membrane electroporation: A minireview of our present (lack of ?) knowledge," *Biochim. Biophys. Acta.*, vol. 1724, pp.270-280, Aug. 2005.
- [4] D. Miklavčič, and M. Puc., "Electroporation," in *Wiley Encyclopedia of Biomedical Engineering*, M. Akay, New York: John Wiley & Sons Inc., 2006, pp. 1-11.
- [5] K. Kinoshita, and T. Y. Tsong, "Formation and resealing of pores of controlled sizes in human erythrocyte membranes," *Nature*, vol. 268, pp.438-443, Aug. 1977.
- [6] T. Kotnik, F. Bobanović, and D. Miklavčič, "Sensitivity of transmembrane voltage induced by applied electric field – a theoretical analysis," *Bioelectrochemistry*, vol. 43, pp.285-291, Aug. 1997.
- [7] W. M. Arnold, R. K. Schmutzler, A. G. Schmutzler, H. van der Ven, S. Al-Hasani, D. Krebs, and U. Zimmermann, "Electro-rotation of mouse oocytes: single-cell measurements of zona-intact and zona-free cells and of the isolated zona pellucida," *Biochim. Biophys. Acta.*, vol.904, pp.454-464, Dec. 1987.
- [8] M. Schmeer, T. Seipp, S. Kakorin, and E. Neumann, "Mechanism for the conductivity changes caused by membrane electroporation of CHO cell-pallets," *Phys. Chem. Chem. Phys.*, vol.6, pp.5564-5574, Nov. 2004.
- [9] M. Hibino, H. Itoh, and K. Kinoshita Jr., "Time courses of cell electroporation as revealed by submicrosecond imaging of transmembrane potential," *Biophys. J.*, vol.64, pp.1789-1800, Jun. 1993.
- [10] M. Pavlin, and D. Miklavčič, "Effective conductivity of a suspension of permeabilized cells: a theoretical analysis," *Biophys. J.*, vol. 85, pp.719-729, Aug. 2003.
- [11] M. Pavlin, K. Maša, M. Reberšek, G. Pucihar, F. X. Hart, R. Magjarević, and D. Miklavčič, "Effect of cell electroporation on the conductivity of a cell suspension," *Biophys. J.*, vol. 88, pp.4378-4390, Jun. 2005.
- [12] R. P. Joshi, Q. Hu, and K. H. Schoenback, "Improved energy model for membrane electroporation in biological cells subjected to electrical pulses," *Phys. Rev. E.*, vol. 65, pp.041920-1-041920-8, Apr. 2002.
- [13] V. F. Pastushenko, Y. A. Chizmadzhev, and V. B. Arakelyan, "Electric breakdown of bilayer lipid membranes II. Calculation of the membrane lifetime in the steady-state diffusion approximation," *Bioelectrochemistry*, vol. 6, pp.53-62, Aug. 1979.
- [14] J. H. Kroeger, D. Vernon, and M. Grant, "Curvature-drive pore growth in charge membrane during charge-pulse and voltage-clamp experiments," *Biophys. J.*, vol. 96, pp.907-916, Feb. 2009.
- [15] J. C. Neu, and W. Krassowska, "Asymptotic model of electroporation," *Phys. Rev. E*, vol. 59, pp.3471-3482, Mar. 1999.
- [16] R. W. Glaser, S. L. Leikin, L. V. Chernomordik, V. F. Pastushenko, and A. I. Sokirko, "Reversible electrical breakdown of lipid bilayers: formation and evolution of pores," *Biochim. Biophys. Acta.*, vol. 940, pp.275-287, May 1988.
- [17] A. Ramos, D. O. H. Suzuki, and J. L. B. Marques, "Numerical simulation of electroporation in spherical cells," *Artificial Organs*, vol. 28, pp.357-361, Apr. 2004.
- [18] A. Ramos, "Effects of the electroporation in the field calculation in biological tissues," *Artificial Organs*, vol. 29, pp.510-513, Jun. 2005.
- [19] K. Kinoshita, I. Ashikawa, N. Saita, H. Yoshimura, H. Itoh, K. Nagayama, and A. Ikegami, "Electroporation of cell membrane visualized under a pulsed-laser fluorescence microscope," *Biophys. J.*, vol. 53, pp. 1015-1019, Jun. 1988.
- [20] K. A. DeBruin, and W. Krassowska, "Modeling electroporation in a single cell. i. effects of field strength and rest potential," *Biophys. J.*, vol. 77, pp. 1213-1224, Sep. 1999.
- [21] Z. Vasilkoski, A. T. Esser, T. R. Gowrishankar, and J. C. Weaver, "Membrane electroporation: the absolute rate equation and nanosecond time scale pore creation," *Phys. Rev. E.*, vol. 021904, pp.1-12.
- [22] W. Krassowska, and P. D. Filev, "Modeling electroporation in a single cell," *Biophys. J.*, vol. 92, pp.404-417, Jan. 2007.
- [23] C. Wilhelm, M. Winterhalter, U. Zimmermann, and R. Benz, "Kinetic of pore size during irreversible electrical breakdown of lipid bilayer membranes," *Biophys. J.*, vol. 64, pp.121-128, Jan. 1993.
- [24] K. Asami, Y. Takahashi, and S. Takashima, "Dielectric properties of mouse lymphocytes and erythrocytes," *Biochim. Biophys. Acta.*, vol. 1010, pp.49-55, 1989.
- [25] J. C. Neu, K. C. Smith, and W. Krassowska, "Electrical energy required to form large conducting pores," *Bioelectrochemistry*, vol. 60, pp.107-114, Aug. 2003.
- [26] H. Leontiadou, A. E. Mark, and S. J. Marrink, "Molecular dynamics simulations of hydrophilic pores in lipid bilayer," *Biophys. J.*, vol. 86, pp.2156-2164, Apr. 2004.
- [27] J. T. Gimsa, H. Schnelle, G. Zechel, and R. Glaser, "Dielectric spectroscopy of human erythrocytes: investigations under the influence of nystatin," *Biophys. J.*, vol. 66, pp.1244-1253, Apr. 1994.
- [28] A. Ramos, D. O. H. Suzuki, and J. L. B. Marques, "Numerical study of the electrical conductivity and polarization in a suspension of spherical cells," *Bioelectrochemistry*, vol. 68, pp.213-217, May 2006.
- [29] M. Pavlin, T. Slivnik, and D. Miklavčič, "Effective conductivity of cell suspension," *IEEE Trans. Biom. Eng.*, vol. 49, pp.77-80, Jan. 2002.
- [30] R. Susil, D. Semrov, and D. Miklavčič, "Electric field-induced transmembrane potential depends on cell density and organization," *Electro-Magnetobiol.*, vol. 17, 391-399, Nov. 1998.
- [31] C. Barrau, J. Teissié, and B. Gabriel, "Osmotically induced membrane tension facilitates the triggering of living cell electroporation," *Bioelectrochemistry*, vol. 63, pp.327-332, Jun. 2004.
- [32] I. G. Abidor, L. -H. LI, S. W. HUI, "Studies of cell pellets: II. Osmotic properties, electroporation, and related phenomena: membrane interactions," *Biophys. J.*, vol. 67, pp. 427-435, Jul. 1994.
- [33] L. V. Chernomordik, S. I. Sukharev, S. V. Popov, V. F. Pastushenko, A. V. Sokirko, I. G. Abidor, and Y. A. Chizmadzhev, "The electrical breakdown of cell and lipid membranes: the similarity of phenomenologies," *Biochim. Biophys. Acta.*, vol. 902, pp. 360-373, Sep. 1987.
- [34] J. Teissié, and M. P. Rols, "An experimental evaluation of the critical potential difference inducing cell membrane electroporation," *Biophys. J.*, vol. 65, pp.409-413, Jul. 1993.
- [35] G. Pucihar, T. Kotnik, M. Kandušer, and D. Miklavčič, "The influence of medium conductivity on electroporation and survival of cells in vitro," *Bioelectrochemistry*, vol. 54, pp.107-115, Nov. 2001.
- [36] S. Kakorin, and E. Neumann, "Ionic conductivity of electroporated lipid bilayer membrane," *Bioelectrochemistry*, vol. 56, pp.163-166, May 2002.
- [37] D. A. Stewart, T. R. Gowrishankar, and J. C. Weaver, "Transport lattice approach to describing cell electroporation: use of a local asymptotic model," *IEEE Transactions on Plasma Science*, vol. 30, pp.1696-1708, Aug. 2004.
- [38] C. Wilhelm, M. Winterhalter, U. Zimmermann, and R. Benz, "Kinetic of pore size during irreversible electrical breakdown of lipid bilayer membranes," *Biophys. J.*, vol. 64, pp.121-128, Jan. 1993.
- [39] J. H. Kroeger, D. Vernon, and M. Grant, "Curvature-drive pore growth in charge membrane during charge-pulse and voltage-clamp experiments," *Biophys. J.*, vol. 96, pp.907-916, Feb. 2009.
- [40] D. C. Chang, and T. S. Reese, "Changes in membrane structure induced by electroporation as revealed by rapid-freezing electron microscopy," *Biophys. J.*, vol. 58, pp.1-12, Jul. 1990.
- [41] H. Ohshima, "Electrical conductivity of a concentrated suspension of spherical colloidal particles," *J. Colloid Interface Sci.*, vol. 212, pp. 443-448, Apr. 1999.
- [42] F. Carrique, F. J. Arroyo, and A. V. Delgado, "Electrokinetics of concentrated suspensions of spherical colloidal particles: effect of a dynamic Stern layer on electrophoresis and DC conductivity," *J. Colloid Interface Sci.*, vol. 243, pp.351-361, Oct. 2001.
- [43] A. Yaari, "Mobility of human red blood cells of different age group in an electric field," *Blood*, vol. 33, pp.159-163, Feb. 1969.
- [44] A. Van de Wal, M. Minor, W. Norde, A. J. B. Zehnder, and J. Lyklema, "Conductivity and dielectric dispersion of gram-positive bacterial cells," *J. Colloid Interface Sci.*, vol. 186, pp.71-79, Feb. 1997.



**Daniela O. H. Suzuki** was born in 1973. She received graduate degree in electrical engineering in 1996 and PhD. degree in electrical engineering in 2009 from the Federal University of Santa Catarina (UFSC), Florianópolis-SC, Brazil. Her current interests include modeling biological processes, experimental, and numerical investigation of membrane electroporation, electrophysiological phenomena.

**Airton Ramos** received graduate degree in electrical engineering in 1987 from State University of Santa Catarina (UDESC), Joinville-SC, Brazil and PhD. degree in electrical engineering in 2003 from the Federal University of Santa Catarina (UFSC), Florianópolis-SC, Brazil. He is currently an Assistant Professor at UDESC. His research interests include modeling the biological phenomena, developing numerical methods for bioelectromagnetics and bioimpedance.

**Maria C. M. Ribeiro** received graduate degree in biological science in 1979 from State University of Mogi das Cruzes and PhD. degree in genetics from the State University of São Paulo, São Paulo, Brazil, in 1988. She was a Postdoctoral Fellow from 1989 to 1991 at Oncocentro Foundation, São Paulo, and from 1994 to 1996 at State University of São Paulo. She is researching and teaching as Assistant Professor at the Federal University of Santa Catarina since 1996. Her current interests are human and molecular genetics.

**Luisa H. Cazarolli** received the graduate degree in pharmacy degree in 2003 from Federal University of Universidade Federal de Santa Maria, Santa Maria-RS, Brazil, and the PhD. degree in pharmacy from the Federal University of Universidade Federal de Santa Catarina, Florianópolis-SC, Brazil, in 2009. She is currently a Postdoctoral Fellow in the chemistry department at Federal University of Santa Catarina. Her current interests are physiologic and biochemical alterations in cells.

**Fátima R. M. B. Silva** received graduate degree in chemistry degree in 1984 from Catholic University of Pelotas, Pelotas-RS, Brazil, and PhD. degree in biochemistry from the Federal University of Rio Grande do Sul, Porto Alegre-SC, Brazil, in 1995. She is researching and teaching as Assistant Professor at the Federal University of Santa Catarina since 1994. Her current interests are physiologic and biochemical alterations in cells.

**Laura D. Leite** received bachelor degree in 1979 in pharmacology at University of California, Santa Barbara, USA, and PhD. degree in physiology from the Federal University of do Rio Grande do Sul, Porto Alegre-SC, Brazil, in 1998. She is researching and teaching as Assistant Professor at the Federal University of Santa Catarina since 1995. Her current interests are human physiology and electrophysiology.



**Jefferson L. B. Marques** received graduate degree in electrical engineering in 1985 from Federal University of Santa Maria, Santa Maria-RS, Brazil, and PhD. degree in medical physics and clinical engineering in 1994 from the University of Sheffield, Sheffield, UK. He is currently an Associate Professor at the Federal University of Santa Catarina. His research interests include mathematical modeling of physiological phenomena, biomedical instrumentation, and digital signal processing.